JOURNAL

OF THE AMERICAN CHEMICAL SOCIETY

VOLUME 106, NUMBER 2 JANUARY 25, 1984

Laser pH-Jump Initiated Proton Transfer on Charged Micellar Surfaces

Mario J. Politi and Janos H. Fendler*

Contribution from the Department of Chemistry and Institute of Colloid and Surface Science, Clarkson College of Technology, Potsdam, New York 13676. *Received July 15, 1983*

Abstract: Proton-transfer processes involving 8-hydroxy-1,3,6-pyrenetrisulfonate (POH), bromocresol green, bromophenol red, bromothymol blue, and theymol blue have been investigated by steady-state and subnanosecond time-resolved fluorescence techniques as well as by laser pH jump in water and in aqueous cationic micellar solutions. In the laser-initiated pH jump, advantage has been taken of the very much stronger acidity of POH in the excited singlet than in the ground state; pK = 7.2, $pK^* \simeq 0.5$ both in water and in micellar hexadecyltrimethylammonium bromide (CTAB). Excitation of POH by a 8–10-ns, 353-nm, 2–5 mJ laser pulse in the pH 4–7 range resulted in the formation of $(1–3) \times 10^{-6}$ M H^+. In the absence of added proton acceptors, rates of PO^- reprotonation, k_{on}, could be measured by laser flash photolysis. Rates of $(5.7 \pm 1.4) \times 10^{10}$, $(4.05 \pm 1.06) \times 10^9$, and $(8.08 \pm 1.30) \times 10^9$ M^{-1} s^{-1} have been determined for k_{on} in 0.01 M NaCl in the absence and in the presence of 8.0×10^{-3} M CTAB and hexadecyltrimethylammonium chloride (CTACl), respectively. The laser pH-jump ejected proton could be transferred to suitable acceptor dyes. In water only initial velocities could be measured for this process, governed by $k_{on}^{D'}$. The rate for the subsequent step, the deprotonation of the protonated dye, governed by $k_{off}^{D'}$, could, however, be determined more precisely. $k_{on}^{D'}$ values were then calculated from the pK_a's of the dye, determined in water and in aqueous micelles. $k_{off}^{D'}$ and $k_{on}^{D'}$ were found to be less than an order of magnitude and up to 55-fold smaller in micelles than in water. Interestingly, micelles dramatically altered the proton-transfer behavior of bromophenol red and bromothymol blue. At appropriate pH values PO^- protonation by the protonated form of the indicator could be observed and $k_{on}^{D''}$ could be measured directly. Such behavior could not be realized in water. Steady-state and subnanosecond time-resolved fluorescence spectroscopy indicated the incomplete deprotonation of $(POH)^*$ in the micellar environments in the pH 3–7 region. Rate constants for $(PO^-)^*$ formation, k^*_{off}, have been determined to be $(4.8–8.9) \times 10^9$ and 4.8×10^8 s^{-1} in 0.01 M NaCl in the absence and in the presence of aqueous micelles, respectively. Dynamic laser light scattering showed that the size of micelles ($\simeq$50 Å diameter) remained unaffected by the addition of the proton donors and acceptors used. These results are discussed in terms of charged micellar effects on proton transfer.

Introduction

Proton transfer is one of the most fundamental chemical reactions.[1,2] Protons are involved in acid–base equilibria and are implicated in Mitchell's chemiosmotic hypothesis.[3–5] The recently developed laser-induced pH-jump technique provides a means for the direct determination of proton-transfer rates.[6–16] This technique utilizes a proton donor which is a very much stronger acid in its singlet excited state than in its ground state (i.e., $pK^* << pK$). Excitation by a strong (1–10 mJ) but short (2–15-ns) laser pulse at a suitable pH ($pK^* < pH < pK$) results in proton ejection. The ejected proton can, in turn, react with appropriate indicators. Fast detection techniques allows the monitoring of proton transfer in the microsecond time domain.[6–16] Electrolytes, solvents, and biomacromolecules are known to alter proton-transfer rates and equilibria.[17] An understanding of these effects is

(1) Bell, R. P. "The Proton in Chemistry", 2nd ed.; Methuen Inc.: New York, 1973.
(2) Caldin, E. F.; Gold, V. "Proton-Transfer Reactions"; Methuen Inc.: New York, 1975.
(3) Mitchell, P. "Chemiosmotic Coupling in Oxidative and Photosynthetic Phosphorylation", and "Chemiosmotic Coupling and Energy Transduction", Glynn Research: Bodmin, Cornwall, U.K., 1966, 1968.
(4) Boyer, P. D.; Chance, B.; Ernster, L.; Mitchell, P.; Racker, E.; Slater, E. C. *Annu. Rev. Biochem.* **1977**, *46*, 955–1026.
(5) Nicholls, D. G. "Bioenergetics. An Introduction to the Chemiosmotic Theory"; Academic Press: New York, 1982.
(6) Gutman, M.; Nachliel, E.; Gerhson, E.; Giniger, R.; Pines, E. *J. Am. Chem. Soc.* **1983**, *105*, 2210–2216.
(7) Smith, K. K.; Kaufmann, K. J.; Huppert, D.; Gutman, M. *Chem. Phys. Lett.* **1979**, *64*, 522–527.
(8) Campillo, A. J.; Clark, J. H.; Shapiro, S. L.; Winn, K. R. In "Picosecond Phenomena", Proceedings of the First International Conference on Picosecond Phenomena, May 24–26, 1978 (Springer Series in Chemical Physics) Shank, C. V., Ippen, E. P., Shapiro, S. L., Eds.; Springer-Verlag: Berlin, 1978; Vol. 4, pp 319–326.
(9) Clark, J. H.; Shapiro, S. L.; Campillo, A. J.; Winn, K. R. *J. Am. Chem. Soc.* **1979**, *101*, 746–748.
(10) Gutman, M.; Huppert, D. *J. Biochem. Biophys. Methods* **1979**, *1*, 9–19.
(11) Huppert, D.; Gutman, M.; Kaufmann, K. J. *Adv. Chem. Phys.* **1981**, *47*, 643–679.
(12) Gutman, M.; Huppert, D.; Pines, E. *J. Am. Chem. Soc.* **1981**, *103*, 3709–3713.
(13) Huppert, D.; Kolodney, E. *Chem. Phys.* **1981**, *63*, 401–410.
(14) Gutman, M.; Huppert, D.; Pines, E.; Nachliel, E. *Biochim. Biophys. Acta* **1981**, *642*, 15–26.
(15) Gutman, M.; Huppert, D.; Nachliel, E. *Eur. J. Biochem.* **1982**, *121*, 637–642.
(16) Huppert, D.; Kolodney, E.; Gutman, M.; Nachliel, E. *J. Am. Chem. Soc.* **1982**, *104*, 6949–6953.

0002-7863/84/1506-0265$01.50/0

required for the interpretation of proton transfer in complex biochemical processes. Micellar effects on indicator equilibria have provided much insight into the effects of electrostatic and hydrophobic interactions.[18] Rate constants for bromocresol green protonation and deprotonation, determined by the laser pH-jump technique, were found to be substantially influenced by neutral Tween 80, Triton X-100, and Brij 58 micelles.[14] Protonation rate constants in mixed Brij 58 and sodium dodecyl sulfate micelles varied with the effective micellar charge as predicted by Debye's equation for diffusion-controlled reactions.[14] Attention has been focused in the present work on the influence of positively charged surfaces on proton-transfer rates and equilibria. Cationic micellar hexadecyltrimethylammonium bromide (CTAB) was used to provide medium for proton transfer involving 8-hydroxy-1,3,6-pyrenetrisulfonate (POH), bromocresol green, bromophenol red, bromothymol blue, and thymol blue.

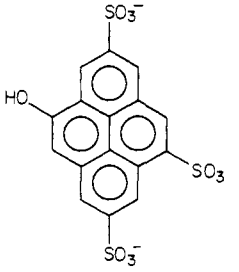

POH

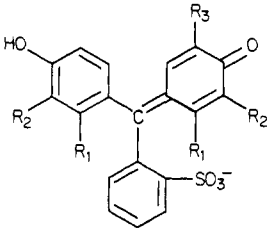

bromocresol green	$R_1 = CH_3$; $R_2 = R_3 = Br$
bromophenol red	$R_1 = R_2 = H$; $R_3 = Br$
bromothymol blue	$R_1 = H$; $R_2 = R_3 = Br$
thymol blue	$R_1 = CH_3$; $R_2 = H$; $R_3 = i\text{-}C_3H_7$

In addition to the expected rate retardations by electrostatic repulsions, a dramatic *change in the direction* of laser-initiated *proton flow* has been observed. Steady-rate and subnanosecond time-resolved fluorescence spectroscopy and dynamic laser light scattering have been utilized to substantiate the interpretation.

Experimental Section

Trisodium 8-hydroxy-1,3,6-pyrenetrisulfonate (POH (Eastman)), was recrystallized three times from aqueous acetone (5:95, v/v) using charcoal.[19] Thin layer chromatography on Merck G-F 254 plates showed only one spot (n-C_4H_9OH : H_2O = 6:1, v/v, as eluent). Tetrabromo-m-cresolsulfonephthalein (bromocresol green (MCB)), dibromophenolsulfonephthalein (bromophenol red (J. T. Baker)), dibromothymolsulfonephthalein (bromothymol blue (MCB or Aldrich)), and thymolsulfonephthalein (thymol blue (Allied Chemical)) were purified by the established method.[20] Typically, 0.5 g of the dye was dissolved in cold, saturated aqueous $NaHCO_3$, the solution was filtered, and the filtrate was slowly neutralized by HCl (to ca. pH 1). The precipitate was filtered, washed with HCl (1.0 M), and dried under vacuum over NaOH for at least 24 h. Hexadecyltrimethylammonium bromide (CTAB (Merck)) was recrystallized three times from acetone:ethanol = 85:15, v/v, and dried under vacuum; hexadecyltrimethylammonium chloride (CTACl (Eastman)) was used as received. All other chemicals used were the best available reagent grade.

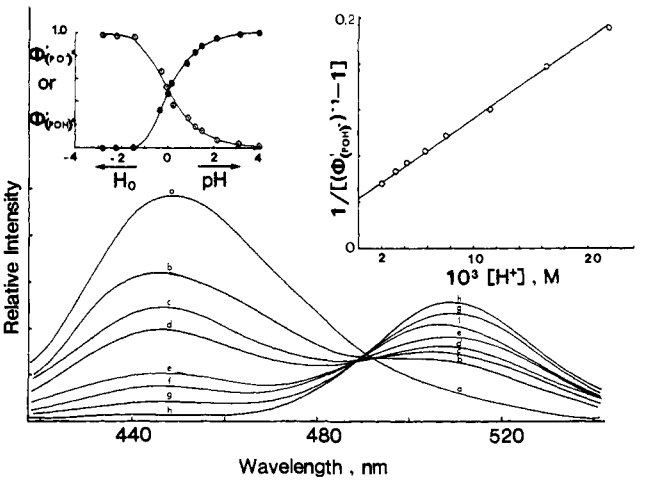

Figure 1. Relative intensity vs. emission wavelength of 1.8×10^{-5} M POH fluorescence in aqueous 0.01 M NaCl at 30 °C in the presence of 3.0, 6.0, and 9.0 (a), 2.0 (b), 1.0 (c), 0.5 (d), 0.67 (e), 0.033 (f), 0.0067 (g), and 0.00067 N (h) H_2SO_4: excitation wavelength, 403 nm, using 1.6- and 2.0-nm slits; uncorrected spectra observed at 90°, (number of other emissions have been recorded at different acidities but are not shown in the figure). Left-hand-side insert shows plots of relative fluorescence quantum efficiencies of (POH)* (⊙) and (PO^-)* (●) as functions of hydrogen ion concentration. The right-hand-side insert plots the data (using values determined between (2 and 20) $\times 10^{-3}$ M H^+, i.e., between e and h) according to eq 1.

Deionized water was doubly distilled in an all-glass apparatus. The final stage of distillation included a superheated oxygenated quartz column. Additionally, double-distilled water was filtered through a 0.2 × Millistak Filter System (Millipore Corp.).

A Radiometer M26 pH meter equipped with a Fisher combination microelectrode was used to determine the hydrogen ion concentration of solutions at ambient temperature. HCl (or H_2SO_4) and NaOH were used to adjust the pH to the required value. Absorption and turbidity measurements were obtained on a Cary 118C spectrophotometer. Fluorescence spectra were recorded on a Spex Fluorolog spectrofluorometer.

Nanosecond laser flash photolysis was carried out with a Quanta-Ray DCR Nd:YAG laser by using the third harmonic (353 nm) line, delivering 8–10-ns pulses at 1–25 mJ per pulse. Details of the laser flash photolysis instrument have been described previously.[21]

Dynamic light-scattering experiments were carried out using a Malvern M-200 goniometer digital correlator intercolor terminal system with a 12-W Spectra Physics 171 argon ion laser. Filtered samples were thermostated at 25 °C in the Malvern cell compartment. Time windows of 0.3–1.0 μs were typically used to obtain no less than 10^7 total counts for autocorrelation. Cumulants were obtained by the software developed by Malvern (now Brookhaven Instrument Co.). Reproducibility of the data was based upon obtaining a Q factor less than 0.3 (±10%).

Fluorescence lifetimes and time-resolved fluorescence anisotropies were determined on a single photon counting system using tunable laser pulses as the excitation source. A Spectra-Physics cavity dumped rhodamine 6G dye laser, syncronously pumped by a mode locked argon ion laser (no. 171), was used to provide tunable 15-ps pulses at 4 MHz. The second harmonic (296 nm, vertically polarized) was generated by means of a temperature-tuned ADA crystal. The residual 592-nm radiation was removed by a 7-54 Corning glass cutoff filter. The ORTEC 457 TAC was used in the normal mode. The "start" signal was obtained from a portion of the 592-nm pulses via a Texas Instrument TIED 56 photodiode and an ORTEC 436 discriminator. The emission signal, viewed at 90° and passed through an ultraviolet Polacoat polarizer (OM type 105, UV WRMR) set at 54.7° for lifetime and 0° ($I_{\parallel}(t)$) or 90° ($I_{\perp}(t)$) for anisotropy determinations, was used to activate the TAC. Photon counting and data treatment by the Marquardt algorithm have been previously described.[22] Precision of the fit was estimated by the χ^2 parameter and by inspecting the residuals and matrix covariances.

(17) Fendler, J. H. "Membrane Mimetic Chemistry", Wiley-Interscience: New York, 1982.
(18) Fendler, J. H.; Fendler, E. J. "Catalysis in Micellar and Macromolecular Systems", Academic Press: New York, 1975.
(19) Kano, K.; Fendler, J. H. *Biochim. Biophys. Acta* **1978**, *504*, 289–299.
(20) Orndorff, W. R.; Sherwood, F. W. *J. Am. Chem. Soc.* **1923**, *45*, 486–500.
(21) Calvo-Perez, V.; Beddard, G. S.; Fendler, J. H. *J. Phys. Chem.* **1981**, *85*, 2316–2319.
(22) Weller, A. *Z. Phys. Chem. (Frankfort am Main)* **1958**, *17*, 224–245. Weller, A. *Prog. Reaction Kinet.* **1969**, *1*, 189–214. Robbins, R. J.; Fleming, G. K.; Beddard, G. S.; Robinson, G. W.; Thistlethwaite, P. J. *J. Am. Chem. Soc.* **1980**, *102*, 6271–6279. Beddard, G. S.; Fleming, G. R.; Porter, G.; Robbins, R. *Phil. Trans. R. Soc. London, Ser. A* **1980**, *298*, 321–334.

Table I. Fluorescence Lifetimes of 1.8×10^{-5} M POH in Aqueous 0.01 M NaCl in Different Media[a]

media	acidity or pH[b]	observation wavelength, ns	τ_1,[c] ns	%	τ_2,[c] ns	%	χ^2 [d]
water	2.84 N HCl	445	0.12	4	5.21	96	3.03
	2.84 N HCl	510			5.21		2.81
	2.84 N HCl	510	0.38		5.21	99	2.50
	1.06	445	0.15	6	5.61	94	4.51
	1.06	510	0.15	4	5.64	96	3.05
	1.50	445	0.13	10	5.77	90	2.89
	1.50	510			5.66		3.17
	1.80	445	0.06	11	5.75	89	2.78
	1.80	510			5.79		1.86
	2.09	445	0.16	20	5.77	80	4.09
	2.09	510			5.85		2.99
	2.84	445			5.10		3.38
	2.84	510			5.89		3.41
	11.22	445			6.04		3.76
	11.22	510			5.89		3.41
8.2×10^{-3} M CTAB	0.54	435	1.14	27.5	3.98	72.5	2.92
	0.54	510			5.24		3.73
	2.84	435	2.29				1.66
	2.84	525			5.25		0.68
	2.84	525			6.98		2.39
	3.08	435	2.08				1.98
	3.08	525			6.76		2.53
	8.07	435	2.11				1.67
	8.07	435	2.16	17	4.64	83	3.51
	8.07	435	2.07	17	4.39	83	3.37
	8.07	525	2.38	17	6.02	83	2.38
	10.87	525			6.04		4.46
8.1×10^{-3} M CTACl	2.81	435	1.88	65	4.86	35	3.07
	2.81	435	2.14				1.96
	2.81	525			5.58		0.95
	2.81	435	2.42				4.19
	2.81	525			7.46		2.45
	2.81	525			6.95		1.68

[a] Determined at ambient temperature. The instrument response time is 300 ps. Values close to these, naturally, have greater errors than those obtained on longer time scales. See ref 12. [b] Using HCl and NaOH to adjust pH. [c] Defined as $I(t) = A(fe^{-t/\tau_1} + (1-f)e^{-t/\tau_2}) + B$, where A is the amplitude and B the background. Convolution of this equation with shifting between the laser profile and fluorescence was performed as described elsewhere.[11] [d] $\chi^2 = \Sigma_{n=LC}^{n=HC}(\text{obsd} - \text{calcd})^2/(\text{obsd} + 1)/(\text{no. of points} - \text{no. of parameters})$; where HC and LC are the high and low counts in the multichannel analyzer.

Results and Discussion

Fluorescence of POH in Aqueous Solutions. Excitation of 1.8×10^{-5} M aqueous unbuffered POH at 403 nm resulted in fluorescence emission with a maximum at 510 nm. Addition of increasing amounts of H_2SO_4 led to the appearance of a new emission band at 445 nm at the expense of that at 510 nm (Figure 1). The emission band at 510 nm corresponds to the singlet excited state of PO^-, $(PO^-)^*$, and that at 445 nm is due to $(POH)^*$. POH is seen to be a very much stronger acid in the excited state than in the ground state. Plots of relative quantum efficiencies of $(PO^-)^*$ and $(POH)^*$ against acidities indicate an approximate $pK^*_a \simeq 0$ (see left-hand-side insert in Figure 1). The excited-state dissociation constant of POH can be more accurately determined (at relatively low hydrogen ion concentrations to prevent the back reaction, k^*_{on}) by plotting the left-hand side of eq 1 against the hydrogen ion concentration:[22]

$$\frac{1}{(\Phi^r_{(POH)^*})^{-1} - 1} = \frac{1}{\tau k^*_{off}} + \frac{\tau' k^*_{on}}{\tau k^*_{off}}[H^+] \qquad (1)$$

where $\Phi^r_{(POH)^*}$ is the relative quantum efficiency of POH fluorescence at different acidities, τ and τ' are the fluorescence lifetimes of $(POH)^*$ and $(PO^-)^*$, and k^*_{on} and k^*_{off} are rate constants for excited-state protonation and deprotonation related to $-\log(k^*_{off}/k^*_{on}) = pK^*_a$. The right-hand-side insert in Figure 1 shows treatment of the data according to eq 1. The slope and the intercept of this line (correlation coefficient = 0.998) and known values of $\tau = 5.2 \times 10^{-9}$ s and $\tau' = 6.0 \times 10^{-9}$ s (Table I) allowed the calculation of $k^*_{on} = 1.86 \times 10^{10}$ M^{-1} s^{-1}, $k^*_{off} = 8.9 \times 10^9$ s^{-1}, and $pK^* = 0.32$. Our k^*_{off} value is in fair agreement with those obtained by others [2.0×10^9 s^{-1},[10] $(3.2 \pm 2.1) \times 10^{10}$ s^{-1},[7] $(2.0 \pm 1.0) \times 10^{10}$ s^{-1},[11] 1.0×10^{10} s^{-1} [13]].

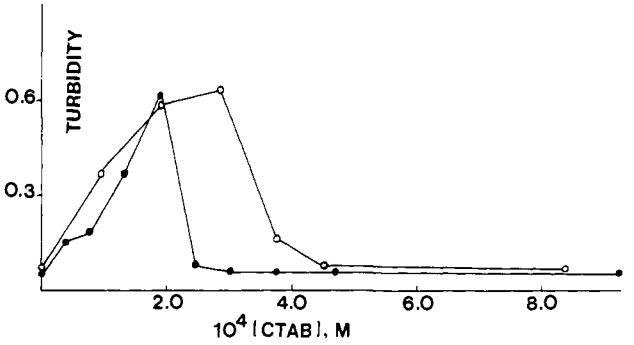

Figure 2. Turbidity vs. CTAB concentration plots for 4.23×10^{-5} M POH at pH 3, measured at 450 nm (●), and for 4.23×10^{-5} M PO^- at pH 11, measured at 350 nm (○).

Fluorescence lifetime determinations have been used to substantiate the data obtained in steady-state measurements. Fluorescence lifetimes of $(POH)^*$, determined in 2.84 N HCl, and $(PO^-)^*$, determined in the high pH region, are 5.2 and 6.0 ns, respectively (Table I).[12] The fluorescence intensity in the low pH region decayed biexponentially at the observation wavelength of 445 nm due to $(POH)^*$. Treatment of the data showed a fast component of decay with ca. 0.2 ns lifetime and a slower component decay at around 6 ns. Contribution of the short component to the overall decay increased with increasing pH within the limits of eq 1.[11] (See right-hand-side insert in Figure 1 and Table I.)

Interaction of Indicators with Micelles. Additions of CTAB to POH (at pH 3) or to PO^- (at pH 11) at 30 °C increased the turbidity of solutions to maximum values at 2×10^{-4} and 3×10^{-4} M CTAB. Further additions of CTAB resulted in sharp decreases

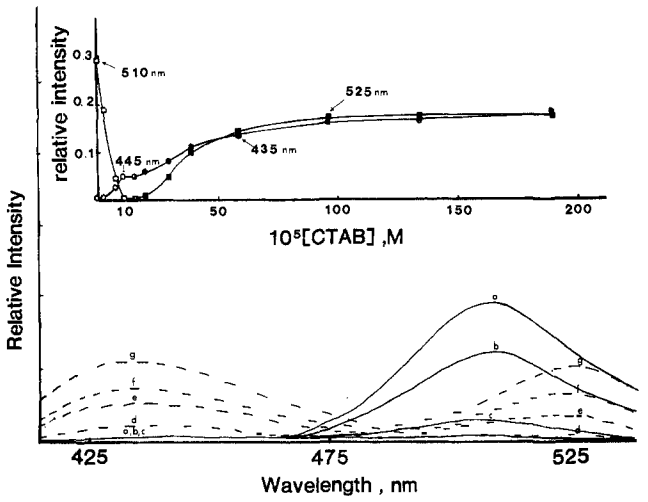

Figure 3. Emission spectra of 2.2×10^{-5} M POH in 0.01 M NaCl at pH 3.2 and 40 °C in the presence of 0 (a), 3.9×10^{-5} (b), 7.8×10^{-5} (c), 1.95×10^{-4} (d), 2.92×10^{-4} (e), 3.89×10^{-4} (f), and 18.87×10^{-4} (g) M CTAB. The insert shows plots of relative fluorescence intensities at 5.10, 445, 435, and 525 nm as a function of CTAB concentration: excitation wavelength, 403 nm; excitation slit, 1.6 nm; emission slit, 2.0 nm; uncorrected spectra observed at 90°.

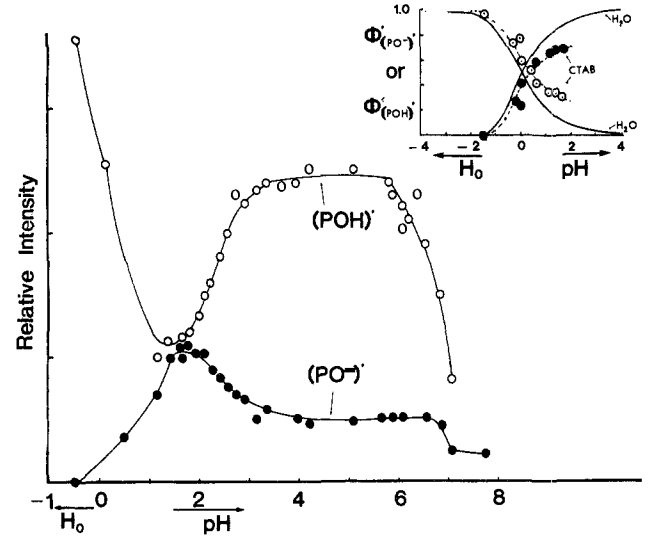

Figure 4. Relative fluorescence spectra of 1.98×10^{-5} M POH in 8.0×10^{-3} M CTAB and 0.01 M NaCl at 30 °C vs. hydrogen ion concentration (pH or H_0): excitation wavelength, 403 nm (slit 1.6 nm); emission wavelength (slit 2.0 nm), 435 nm for (POH)* and 525 nm for (PO^-)* (uncorrected spectra observed at 90 °C). Insert: relative quantum efficiencies of (POH)* (cid) and (PO^-)* (●) as function of acidities in 8.0×10^{-3} M CTAB in the presence of 0.01 N NaCl. Full line is a reproduction of the data in water given in the left-hand insert in Figure 1.

of turbidities to their original values (Figure 2). Fluorescence intensities of 2.2×10^{-5} M POH, observed at 510 nm, pH 3.2, and 40 °C, sharply decreased upon the addition of CTAB below and up to the CMC of the surfactant (Figure 3). Further addition of CTAB, above the CMC, restored the fluorescence intensity roughly to half of its original value but with the maxima shifted to 525 nm. A new fluorescence band with a maximum centered at 435 nm appeared concurrently with the buildup of the 525-nm fluorescence (Figure 3). The insert in Figure 3 shows changes of the relative fluorescence intensities at 510, 525, 445, and 435 nm as functions of added CTAB concentrations. The turbidity and fluorescence data imply the formation of PO^- and POH complexes with some surfactant molecules (below the CMC) and the subsequent solubilization of these complexes by the micelles. Assuming the CMC of CTAB to be 2.0×10^{-4} M[7] in 0.01 M NaCl[18] allowed the assessment of the POH to CTAB micelle

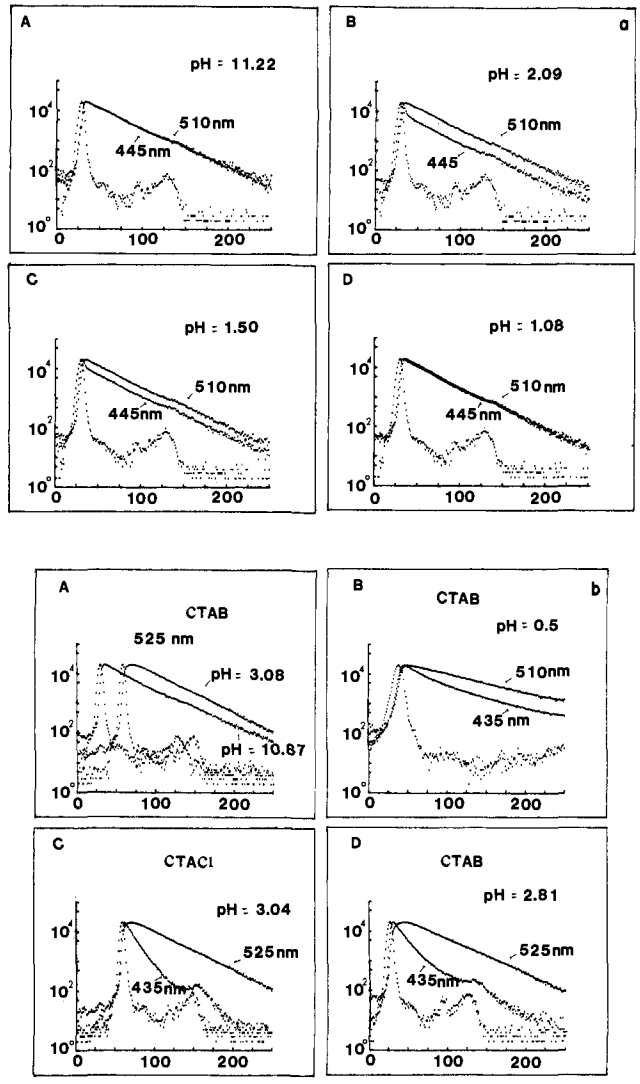

Figure 5. Fluorescence decay plots (intensities vs. channel number at 0.2 ns/channel) of (a) 2.0×10^{-5} M POH in 0.01 M NaCl in water at room temperature: excitation wavelength, 295 nm (emission wavelength and pH values are indicated); (b) 1.8×10^{-5} M POH in 0.01 M NaCl in the presence of 8.0×10^{-3} M surfactant (CTAB or CTACl): excitation wavelength, 295 nm (emission wavelength and pH values are indicated). Scale: 0.2 (A, C, and D) and 0.05 (B) ns/channel.

binding constant to be 1.9×10^4 M^{-1}. This is quite an appreciable binding. The uptake of the POH–surfactant complex by the micelle is clearly seen in the altered emission spectra (Figure 3).

Significantly, addition of micellar CTAB shifted the equilibrium in favor of (POH)*. pH–rate profiles of (POH)* and (PO^-)* fluorescence intensities in 8.0×10^{-3} M CTAB are shown in Figure 4. In the strong acid region (pH <2) the predominant species, just as in water, is (POH)*. Using data in this region allowed the estimation of pK^*_a in 0.01 M NaCl in the presence of 8.0×10^{-3} M CTAB to be approximately 0.3 (see insert in Figure 4). At higher pH values there is a radical departure from the behavior observed in water (compare the left-hand side of the insert in Figure 1 with Figure 4). Excited-state deprotonation of (POH)* is incomplete. In the 3–7 pH region emission intensities of (POH)* and (PO^-)* remain constant! Entirely analogous behavior has been reported previously for the excited-state deprotonation of 1-naphthol in micelles.[23-25] Apparently the local microenvironment around (POH)* is sufficiently different from water to

(23) Klein, V. K. A.; Hauser, M. *Z. Phys. Chem. (Frankfort am Main)* **1975**, *96*, 139–146. Khuanga, V.; McDonald, R.; Selinger, B. K. *Ibid.* **1976**, *101*, 209–224.
(24) Selinger, B. K.; Weller, A. *Aust. J. Chem.* **1977**, *30*, 2377–2381.
(25) Selinger, K. *Aust. J. Chem.* **1977**, *30*, 2087–2090.

Table II. Diffusion Coefficients, D, and Hydrodynamic Diameters, D_H, of Micellar CTAB at 25.0 °C[a]

conditions	angle, deg	$10^7 D$, cm^2 s^{-1}	D_H, Å
0.008 M CTAB, 0.01 M NaCl, pH 10.8	90	10.3 ± 1.0	53 ± 5
0.010-0.020 M CTAB, 0.02 M NaBr[b]	90	10.0 ± 1.0	64.4
0.010-0.050 M CTAB, 0.02-0.03 M NaBr[c]	90	8.26 ± 0.06	59.4
at CTAB cmc, 0.025 M NaBr[d]		7.80 ± 0.2	63 ± 0.5
0.008 M CTAB, 0.01 M NaCl, pH 3.2	90, 75, 60	10.2 ± 1.0	54 ± 5
0.025 M CTAB, 0.01 M NaCl, pH 3.2	90, 65, 55, 50, 45	10.0 ± 1.0	55 ± 5
0.025 M CTAB, 0.01 M NaCl pH 0	90	7.1 ± 1.0	64 ± 4
0.025 M CTAB, 0.01 M NaCl, 5.7×10^{-5} M POH, pH 4.0	90	9.5 ± 1.0	60 ± 5
0.008 M CTAB, 0.01 M NaCl, 8.0×10^{-5} M bromocresol green, pH 6.0	90	10.0 ± 1.0	51 ± 5

[a] Mean of at least four determinations. [b] Taken from ref 16. [c] Taken from ref 17. [d] Taken from ref 18.

Table III. Absorption Maxima, Extinction Coefficients, and pK_a of Indicators in Water and in 8.0×10^{-3} M Micellar CTAB at 25.0 °C[a]

	basic form		acidic form			
indicator	λ_{max}, nm	$10^{-4}\epsilon_{max}$, M^{-1} cm^{-1}	λ_{max}, nm	$10^{-4}\epsilon_{max}$, M^{-1} cm^{-1}	isosbestic point, nm	pK_a
			in water			
bromocresol green	615	3.85	440	1.58	508	4.60 (4.7,[c] 4.9[d])
bromophenol red	575	3.63	436	1.43	487	5.95 (6.2,[c] 6.0[d])
bromothymol blue	615	3.63	430	0.96	496	7.10 (7.0,[c] 7.3[d])
thymol blue	595	3.38	435	1.31	492	8.60 (8.9,[c] 9.2[d])
pyranine[e]	455	2.16	405	2.17	425	7.20
			in CTAB[f]			
bromocresol green	627	3.85	420	1.57	496	3.35 (3.52)[g]
bromophenol red	586	3.93	427	1.49	482	4.90
bromothymol blue	625	3.57	418	1.11	492	6.20
thymol blue	605	3.55	437	1.42	494	8.40
pyranine[e]	455	2.16	405	2.17	415	7.20

[a] Concentrations of indicators used ranged between $(1-4) \times 10^{-5}$ M. [b] Estimated error 0.2. [c] Taken from ref 30. [d] Taken from ref 31. [e] pK_a values were determined both by absorption and by measuring relative emission intensities at 510 nm using excitation at 400 nm (acidic form) and at 450 nm (basic form).[19] [f] In the presence of 0.01 M NaCl. pK_a values in micelles are apparent pK's, of course. [g] Taken from ref 32.

preclude complete dissociation. The extent of dissociation of (POH)* in the pH 3–7 range (ca. 30%) corresponds to the formation of $(PO^-)^*$ and H^+. Excitation of POH in micellar CTAB by a sufficiently strong laser pulse can, therefore, lead to appreciable proton pulses (see below).

Differences between the excited-state behavior of POH dissociation in aqueous and micellar environments also manifest in the observed fluorescence lifetimes (compare Figures 5a and 5b and see Table I).[26] Most striking is the 2.2-ns component in the two exponential decays. Since the fluorescence lifetimes of POH in micelles in strong acids (5.2 ns) and in the alkaline pH region (6.0 ns) are the same as those in water, the 2.2-ns decay is related to reprotonation and/or to the possibility that some protons cannot escape the field of PO^- in the micellar cage.[14] Buildup of fluorescence at 525 nm, due to the formation $(PO^-)^*$, in the lower pH values could also be observed (see, A, C, and D in Figure 5b). No such buildup was observable in water (Figure 5a). Taking appropriate corrections for the laser pulse, a lifetime of 1.8 ± 0.4 ns was calculated for the fluorescence buildup in micellar solutions due to the formation of $(PO^-)^*$. The satisfactory agreement between the lifetimes observed for the decay of (POH)*, 2.2 ns, and the buildup of $(PO^-)^*$, 1.8 ± 0.4 ns, lends credence to our assignment of this process to k^*_{off}. The experimentally obtained value for the decay of (POH)* leads to $k^*_{off} = 4.8 \times 10^8$ s^{-1} in micellar environment. This value is 10-fold slower than that found in water. Proton dissociations are generally discussed in terms of a two-step process. In the present case the first step is the formation of $(PO^-)^*$ and H^+ within a solvation cage, while the escape of the ions from the solvation cage constitutes the second step.[1,2] Aqueous micelles are likely to retard proton ejection from the cage, with the resultant order of magnitude decrease in the k^*_{off} value. Similar retardation of (POH)* deprotonation had been previously noted in alcohols[13] and electrolytes.[16] Using the reported linear relationship between the rate constant of proton ejection from (POH)* and mol % of added ethanol in water[13] as a solvent polarity ruler, we estimate the environment of (POH)* in aqueous micelles to correspond approximately to 20% ethanol. This is a relatively water-like milieu. The faster than measurable (the limit of our detection is 300 ps) anisotropy decay of (POH)* in CTAB micelles is in accord with the highly aqueous environment of (POH)* in the micelles.

Hydrodynamic diameters of CTAB micelles were determined to be 50 Å by dynamic laser light scattering (Table II). This value is in agreement with those reported previously.[27-29] CTAB micelles are seen to exist even in 1.0 M HCl! Importantly, neither POH nor the dyes affected the morphologies of micelles under our experimental conditions.

Table III summarizes the spectral properties of the unprotonated and protonated dyes in water and in CTAB micelles. The apparent dissociation constant of POH is unaffected by the micelle. Conversely, pK_a values of bromocresol green, bromophenol red, bromothymol blue, and thymol blue are decreased in CTAB micelles by up to one unit (Talbe III). Figure 6 illustrates the pK_a determinations of bromocresol green in water and CTAB micelles.

Laser-Initiated pH Jump. Advantage has been taken of the very much stronger acidity of POH in its excited singlet than its ground state (pK = 7.2, pK^* ≃ 0.5) to generate protons in a few nanoseconds by short energetic laser pulses.[7,8-16] Scheme I describes the processes involved. Excitation of 5×10^{-5} M POH by a 5-mJ, 353-nm laser pulse ($h\nu$) produced ca. 3×10^{-6} M (POH)*.

(26) Observation of decays at 510 nm in strongly acidic media is the consequence of reprotonation and/or incomplete spectral resolution. Decay observed at 445 nm in the high pH region is due to incomplete spectral resolution of (POH)* and $(PO^-)^*$ fluorescences.

(27) Dorshow, R.; Briggs, J.; Bunton, C. A.; Nicoli, D. F. *J. Phys. Chem.* **1982**, *86*, 2388–2395.
(28) Briggs, J.; Dorshow, R. B.; Bunton, C. A.; Nicoli, D. F. *J. Chem. Phys.* **1982**, *76*, 775–779.
(29) Corti, M.; DeGiorgio, V. *Chem. Phys. Lett.* **1978**, *53*, 237–241.

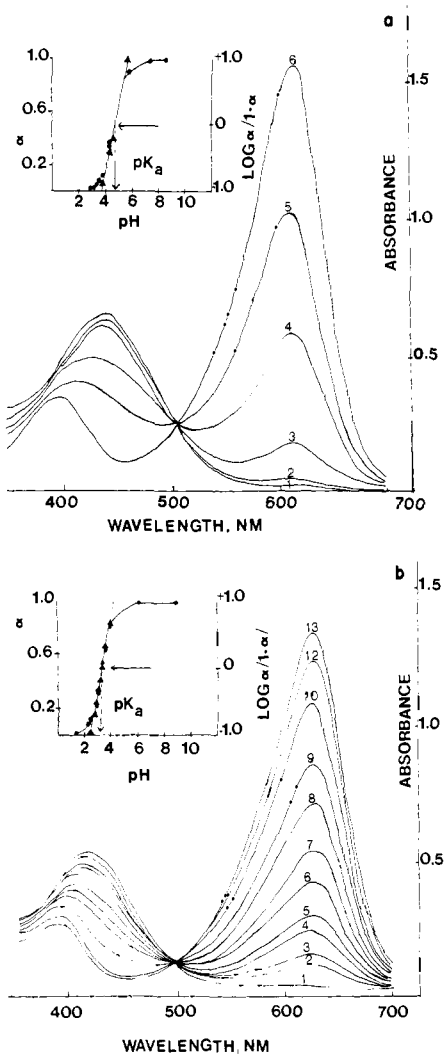

Figure 6. Absorption spectra of (a) 4.12×10^5 M bromocresol green in aqueous 0.01 M NaCl at 25 °C, pH 2.99 (1), 3.04 (2), 3.24 (3), 5.30 (4), 5.76 (5), 7.38 (6) [the insert shows the plot to calculate pK_a values (α is the fraction of the bromocresol green in the basic form)]; (b) 3.43×10^{-5} M bromocresol green in aqueous 0.01 M NaCl in the presence of 8.0×10^{-3} M CTAB at 25.0 °C, pH 6.86 (1), 6.05 (2), 3.82 (3), 3.52 (4), 3.26 (5), 3.12 (6), 2.59 (7), 2.75 (8), 2.63 (9), 2.35 (10), 2.67 (11), 1.38 (12) [the insert shown is used to calculate pK_a values (α is the fraction of bromocresol green in the basic form)].

(POH)* may decay to its ground state by fluorescence (k_f^{POH}) emission at 445 nm and by nonradiative transition (k_{nr}^{POH}). Alternatively, (POH)* may dissociation to $(PO^-)^*$ by a process governed by k^*_{off}. Similarly, the excited-state anion, $(PO^-)^*$, may dissipate its energy by fluorescence emission at 510 nm ($k_f^{PO^-}$), nonradiative transition ($k_{nr}^{PO^-}$), or reprotonation (k^*_{on}). These processes are described by the rate equations:[11]

$$-\frac{d[(POH)^*]}{dt} = (k^*_{off} + k_f^{POH} + k_{nr}^{POH})[(POH)^*] - k^*_{on}[(PO^-)^*][H^+] \quad (2)$$

$$-\frac{d[(PO^-)^*]}{dt} = (k_f^{PO^-} + k_{nr}^{PO^-})[(PO^-)^*] + k^*_{on}[(PO^-)^*][H^+] - k^*_{off}[(POH)^*] \quad (3)$$

Adjusting the pH such that all ground-state population is protonated (say pH 5), integration of eq 2 and 3 leads to

$$[(POH)^*] = [(POH)^*]_0 e^{-t/\tau} \quad (4)$$

$$[(PO^-)^*] = \frac{k^*_{off}[(POH)^*]_0(e^{-t/\tau'} - e^{-t/\tau})}{k^*_{off} - k^*_{on}[H^+] + k_f^{POH} - k_f^{PO^-} + k_{nr}^{POH} - k_{nr}^{PO^-}} \quad (5)$$

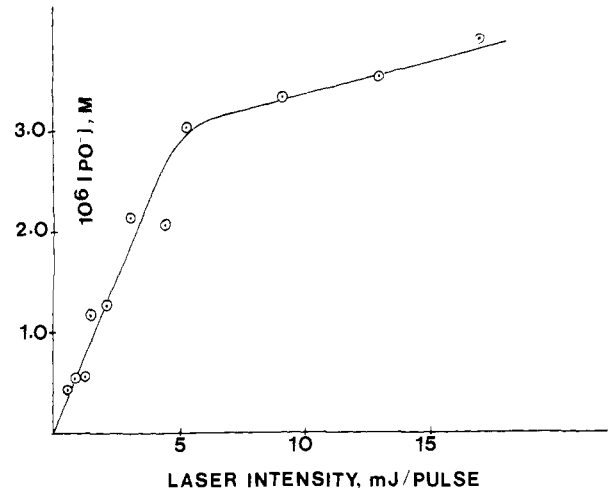

Figure 7. Plot of the (PO^-) concentration produced as a function of the laser intensity.

Scheme I

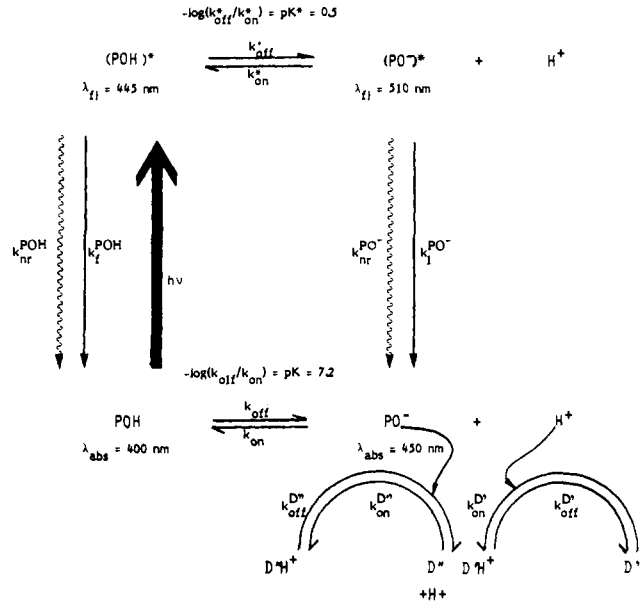

where τ and τ' are the lifetimes of (POH)* and $(PO^-)^*$ at $pK^*_a < pH < pK_a$, and

$$\tau = \frac{1}{k^*_{off} + k_f^{POH} + k_{nr}^{POH}} \quad (6)$$

$$\tau' = \frac{1}{k_f^{PO^-} + k_{nr}^{PO^-}} \quad (7)$$

Fluorescence lifetimes of (POH)* and $(PO^-)^*$ are 5.2 and 6.0 ns, respectively (Table I). Conversely, $k^*_{off} = 8.9 \times 10^9$ s^{-1} (i.e., its half-lifetime is 80 ps). It is seen, therefore, that excitation of POH by a fast laser pulse results in the shifting of the equilibrium in favor of $(PO^-)^*$ and H^+. At the high pH range (say pH 5) the hydrogen ion concentration (bulk H^+ + H^+ generated by laser pulse) is insufficient to protonate $(PO^-)^*$ within its lifetime. The observable net result of POH excitation by a fast laser pulse when $pK^* < pH < pK$ is, therefore, the formation of transient PO^- and H^+.

Excitation of $(2-6) \times 10^{-5}$ M POH in aqueous 0.01 M NaCl in the absence and in the presence of micellar CTAB at a given pH resulted in the bleaching of the ground-state absorbance at 400 nm and in the formation of a transient absorbance due to PO^- at 450 nm (Scheme I). Figure 7 shows the curvilinear dependency of the concentration of the PO^- produced as a function of laser energy. All experiments were carried out in the linear portion

Table IV. Rate Constants for Laser pH-Jump Initiated Protonation of PO^- in Water and in 8.0×10^{-3} M CTAB at 25.0 °C[a]

					In H_2O							
pH	4.69	4.69	4.69	4.82	4.82	5.10	5.10	5.10	5.55	5.55	6.24	6.24
$10^{-10}k_{on}$, M^{-1} s^{-1}	7.12	4.13	5.20	6.30	5.86	6.74	7.53	3.89	6.33	4.15	4.89	6.14
pH	6.53	6.53	7.00	7.00		k_{on}(mean) = 5.74 ± 1.41) × 10^{10} M^{-1} s^{-1} [b]						
$10^{-1}k_{on}$, M^{-1} s^{-1}	6.43	5.87	3.08	8.12								
					In CTAB							
pH	4.10	4.50	4.72	4.72	5.49	5.55	5.55	6.57	6.24	7.11	7.11	
$10^{-9}k_{on}$, M^{-1} s^{-1}	4.27	4.38	3.47	3.81	2.73	2.58	4.12	5.36	4.37	6.02	3.10	
	k_{on}(mean) = (4.05 ± 1.06) × 10^9 M^{-1} s^{-1}; k_{on}(mean) = (8.08 ± 1.30) × 10^9 M^{-1} s^{-1} [c]											

[a] In the presence of 0.01 M NaCl. [POH] = (2–6) × 10^{-5} M. See Scheme I for notations. [b] $k^0_{on} = 1.26 \times 10^{11}$ M^{-1} s^{-1} at $\mu = 0$. [c] Determined in 8.0×10^{-3} M CTACl in the presence of 0.01 M NaCl at 27 °C, pH 5.97. Mean of five determinations.

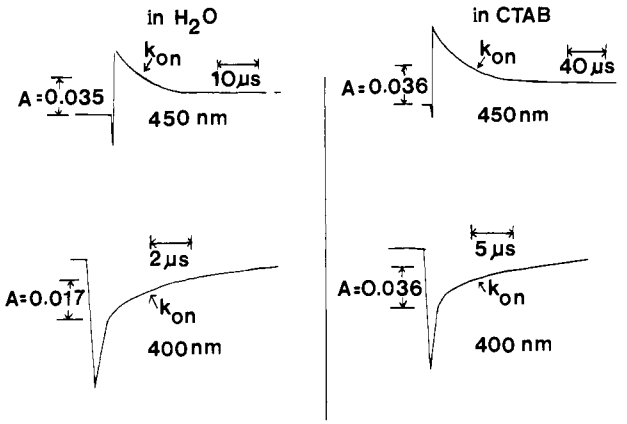

Figure 8. Transient absorbance changes of PO^- (at 450 nm) and POH (at 400 nm) observed following excitation by a 353-nm 8-ns laser pulse in 0.01 M NaCl in the absence and presence 8.0×10^{-3} M CTAB at pH 5.66. Incomplete recovery of 450 nm is the consequence of photoproduct formation. Decreasing laser intensities decreased the buildup of photoproducts.

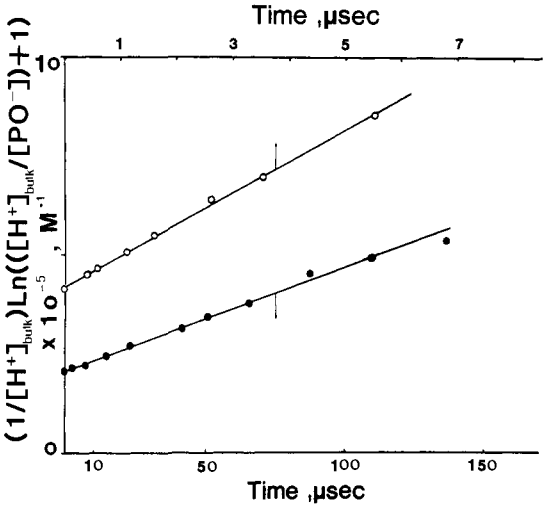

Figure 9. Plot of data according to eq 12 for determing the laser pH-jump initiated proton transfer to PO^- in 0.01 M NaCl in the absence (●) and presence (○) of 8.0×10^{-3} M CTAB.

of excitation, typically at 2 mJ/pulse.

Decay of the absorbance due to PO^-, monitored at 450 nm, paralleled the ground-state recovery of POH, monitored at 400 nm (Figure 8). This process corresponds, of course, to the ground-state protonation of PO^-, governed by k_{on} (Scheme I), expressed by the rate equation:

$$-\frac{d[PO^-]}{dt} = -\frac{d[POH]}{dt} = k_{on}[PO^-][H^+]_t \qquad (8)$$

where $[H^+]_t$, the total hydrogen ion concentration, is the sum of the bulk and ejected hydrogen ion concentrations:

$$[H^+]_t = [H^+]_{bulk} + [H^+]_{ejected} \qquad (9)$$

and, if initially there were only POH (pH < pK − 1), then:

$$[H^+]_{ejected} = [PO^-]_t \qquad (10)$$

and eq 8 becomes

$$-\frac{d[PO^-]}{dt} = k_{on}[PO^-]([PO^-] + [H^+]_{bulk}) \qquad (11)$$

which integrates to

$$-\frac{1}{[H^+]_{bulk}} \ln\left(\frac{[H^+]_{bulk}}{[PO^-]} + 1\right) + C = k_{on}t \qquad (12)$$

Figure 9 shows typical plots of the data according to eq 12, and Table IV summarizes the obtained k_{on} values. Correcting the rate constants in aqueous NaCl for the ionic strength effects, leads to $k^0_{on} = 1.23 \times 10^{11}$ M^{-1} s^{-1} at zero ionic strength, in good agreement with that obtained previously (1.3×10^{11} M^{-1} s^{-1}).[12]

Micellar Effects on PO^- Protonation Equilibria. Figure 8 compares the time dependencies of PO^- protonation, subsequent to the laser pulse initiated proton ejection, in 0.01 M NaCl in the absence and in the presence of 8.0×10^{-3} M micellar CTAB. The absorbance at 450 nm, due to PO^-, is seen to decrease at a considerably slower rate in the environment of the positively charged micelles than in water. Figure 8 shows the rate of POH ground-state recovery, following the pH jump, as monitored at 400 nm. Rates of PO^- depletion nicely parallel the recovery of POH, substantiating the proposed ground-state protonation (eq 8). Figure 9 compares the treatment of the protonation data (according to eq 12) in water with that in micellar CTAB. The obtained rate constant for PO^- protonation in 8.0×10^{-3} M CTAB, $k_{on} = (4.05 - 1.06) \times 10^9$ M^{-1} s^{-1}, is an order of magnitude smaller than that in water (Table IV). Not surprisingly, proton transfer on the positively charged micellar surfaces is substantially reduced, presumably because of the low ionic strengths, local hydrogen ion concentration, and reduced dielectric constant of the interface.

Proton Transfer Involving Indicators in Water. The proton ejected from POH by the fast laser pulse can be transferred to a suitable acceptor dye D′ (Scheme I). Requirements for this transfer are quite stringent.[8-16] The proton donor, POH, must be mainly in the acidic form (i.e., the pH of the solution should be ≤7). Conversely, the indicator, present at sufficient concentrations, should be predominantly in its unprotonated form prior to the pH jump. The concentration of hydrogen ions generated by the laser pulse should be higher than that in the bulk. Under these conditions the indicator equilibrium

$$D' + H^+ \underset{k^{D'}_{off}}{\overset{k^{D'}_{on}}{\rightleftharpoons}} D'H^+ \qquad (13)$$

is perturbed. Following the initial diffusion-controlled protonation, governed by $k^{D'}_{on}$, the time course of equilibrium reestablishment, the deprotonation, can be followed on the microsecond time scale. Figure 10 shows typical transient behaviors of bromocresol green anion absorbance following the injection of protons. The initial bleaching of absorbance due to D′ (observed at 630 nm by using a He–Ne laser as the analyzing light) corresponds to the formation of $D'H^+$. The recovery of ground-state D′ absorbance is a measure of $k^{D'}_{off}$. A similar behavior has been observed on using bromo-

Table V. Rate Constants for the Laser pH-Jump Initiated Proton-Transfer Processes Involving Indicators in Water and in 8.0×10^{-3} M Micellar CTAB at 25.0 °C[a]

indicator[b]	in H_2O		in 8.0×10^{-3} M CTAB		in H_2O	in 8.0×10^{-3} M CTAB
	$k_{off}^{D'}$, s^{-1} [c]	pH range	$k_{off}^{D'}$, s^{-1} [c]	pH range	$k_{on}^{D'}$, M^{-1} s^{-1} [f]	$k_{on}^{D'}$, M^{-1} s^{-1} [f]
bromocresol green	$(2.79 \pm 0.83) \times 10^5$ $(3.16 \pm 6.31) \times 10^5$ [d]	5.60-5.81	4.3×10^5 [e]		1.1×10^{10} 2.4×10^{10} [d]	5.41×10^8 [e]
bromophenol red	$(6.72 \pm 1.7) \times 10^4$	5.57-7.52	$(1.36 \pm 0.24) \times 10^4$	5.22-6.44	5.99×10^{10}	1.1×10^9
bromothymol blue	1.4×10^4 [d]		$(3.50 \pm 1.40) \times 10^3$	6.24-6.56	1.41×10^{11} [d] 2.5×10	6.2×10^9

[a] See Scheme I for notation. [b] Stoichiometric concentrations of indicators ranged between (1 and 4) $\times 10^{-5}$ M. [c] Experimentally determined values. Mean of at least six determinations in the indicated pH range. Each value was obtained by following the buildup of absorbance due to D' (at 615 nm for bromocresol green and bromothymol blue and at 580 nm for bromophenol red). [d] Taken from ref 27. [e] Taken from ref 28. [f] Values calculated from $k_{off}^{D'}/k_{on}^{D} = K_a$ using the pK_a values given in Table III. [g] Taken from ref 13.

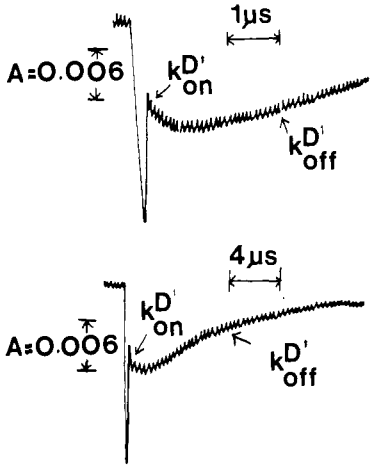

Figure 10. Transient absorbance changes of 2.0×10^{-5} M bromocresol green at 630 nm (using a 5-mW He–Ne laser as the analyzing light source) and pH 6.03 in 0.01 M aqueous NaCl solution following a laser pH-jump initiated proton ejection. [POH] = 3×10^{-5} M.

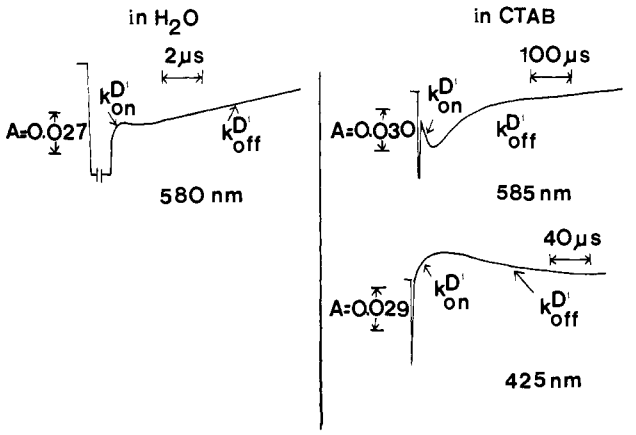

Figure 11. Transient absorbance changes of 3.0×10^{-5} bromophenol red in 0.01 M NaCl at pH 5.55 in the absence and in the presence of 8.0×10^{-3} M CTAB following a laser pH-jump initiated proton ejection. [POH] = 3×10^{-5} M.

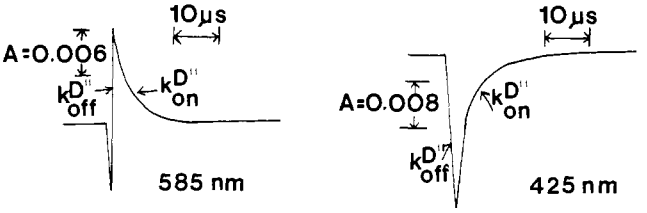

Figure 12. Transient absorbance changes of 3.0×10^{-5} M bromophenol red in 0.01 M NaCl in the presence of 8.0×10^{-3} M CTAB at pH 4.00 following a laser pH-jump initiated proton ejection.

phenol red. Values of $k_{off}^{D'}$ are collected in Table V. Within the stated experimental errors, rate constants for the indicator deprotonation remained independent of the pH. Further, the obtained $k_{off}^{D'}$ value for bromocresol green agreed well with that reported in the literature.[13]

Although protonation rates are often discernible, they are better estimated from the dissociation constants of the indicators (given in Table III). Calculated $k_{on}^{D'}$ values for the protonation of bromocresol green and bromophenol red are given in Table V. These values are in the expected range for diffusion-controlled proton-transfer processes.

Proton Transfer Involving Indicators in CTAB Micelles. Rate constants for protonation and deprotonation of negatively charged indicators are substantially influenced by cationic micellar CTAB. Figure 11 shows typical flash photolytic traces for laser pH-jump initiated proton transfers involving bromophenol red in water and in CTAB micelles. Once again, the deprotonation rates, $k_{off}^{D'}$, are measured more conveniently. The proposed protonation (Scheme I) has been verified for all systems by comparing rates of absorbance changes for D' with $D'H^+$. Such a typical comparison is shown in Figure 11. The transient absorbance changes at 585 nm, due to $D'H^+$, are accurately mirrored by the behavior of D', monitored at 425 nm. The experimentally determined $k_{off}^{D'}$ values in 8.0×10^{-3} M CTAB for the deprotonation of bromophenol red and bromothymol blue are also collected in Table V. Effects of micelles on $k_{off}^{D'}$ are relatively modest. Decreases of less than an order of magnitude are observed. Conversely, the apparent rate constant for proton transfer is up to 55-fold slower in micellar CTAB than that in water (Table V). Once again, these results can be rationalized in terms of electrostatic interactions.

The proton-transfer behavior of bromophenol red in aqueous CTAB micelles at pH 4 (Figure 12) is dramatically different from that at pH 5.5 (Figure 11). The initial step at pH 5.5 corresponds to the rapid proton transfer ($k_{on}^{D'}$). Conversely at pH 4 there is a rapid initial deprotonation as monitored by an increase of absorbance at 585, due to $D'H^+$, and by the bleaching of the ground state at 425 nm, due to D' (Figure 12). Subsequently, protonation of the dye, governed by $k_{on}^{D'}$, becomes observable in the microsecond time scale. This behavior has been rationalized in terms of proton transfer from the acidic form of the dye to PO^- and subsequent dye reprotonation. Modification of eq 13 to

$$D''H^+ + PO^- \xrightarrow{k^{D''}_{off}} D'' + POH \qquad (14)$$

is meant to convey the competitive protonation of PO^- (see Scheme I). In reality $D''H^+ = D'H^+$, $D'' = D'$, and $k_{on}^{D''} = k_{on}^{D'}$. The important consequence of PO^- protonation is that $k_{on}^{D''}$ rather than $k_{off}^{D'}$ becomes the experimentally determined rate constant. Competition between protonations of D' (by H^+) and PO^- (by $D''H^+$) depends on the dissociation constants of POH and $D'H^+$, the relative concentrations of these species, and the pH of the solution. Judicious selection of the appropriate parameters allows a fine tuning of the observed processes. Figure 13 shows changes in the protonation equilibria of bromothymol blue aqueous CTAB micelles at different pH values. At a pH value above the pK_a of bromothymol blue (6.20), transfer of the laser pulse ejected proton to D' is the initial process. This is seen in terms of the decrease of absorbance at 640 nm, due to D' (Figure 13).s At pH 6.20

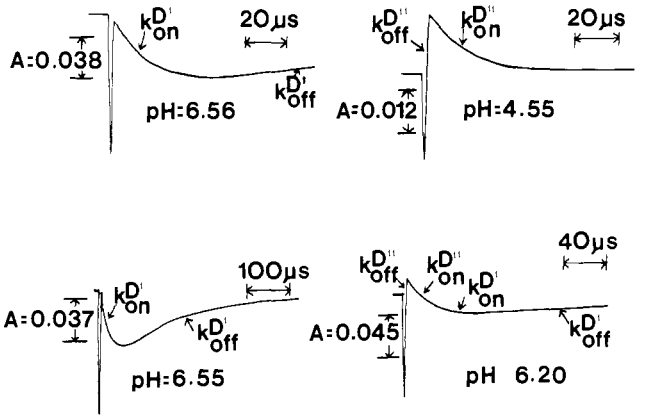

Figure 13. Transient absorbance changes at 640 nm (left-hand-side traces) and at 615 nm (right-hand-side traces) of 4.0×10^{-5} M bromothymol blue in 0.01 M NaCl in the presence of 8.0×10^{-3} M CTAB following a laser pH-jump initiated proton ejection.

Table VI. Rate Constants for Laser pH-Jump Initiated Proton Transfer Involving Indicators in 8.0×10^{-3} M CTAB at 25.0 °C[a]

indicator[b]	pH range	$k_{on}^{D''}$, M^{-1} s^{-1} [c]	$k_{off}^{D''}$, s^{-1} [d]
bromophenol red	3.44-4.45	$(1.61 \pm 0.69) \times 10^9$	2.3×10^4
bromothymol blue	4.54-5.60	$(3.33 \pm 1.0) \times 10^9$	$\times 10^3$

[a] See Scheme I for notations. [b] Stoichiometric concentrations of indicators ranged from (1 to 4) $\times 10^5$ M. [c] Experimentally determined values. Mean of at least six determinations in the indicated pH range. Each value was obtained by following the decay of absorbance due to D'' (at 585 nm for bromophenol red and at 615 nm for bromothymol blue) or the buildup of absorbance due to $D''H^+$ (at 425 nm for bromophenol red and at 418 nm for bromothymol blue). [d] Values calculated from $k_{off}^{D''}/k_{on}^{D'} = K_a$ using the pK_a values given in Table III.

both processes are observable. The small fast initial rise of absorbance at 615 nm, due to the buildup of D'' from $D''H^+$, is attributed to $k_{off}^{D''}$. The subsequent decay is the protonation of D' and D'', governed by $k_{on}^{D'}$ and $k_{on}^{D''}$, followed by a slower recovery of the absorbance by deprotonation, $k_{off}^{D'}$ (Figure 13). At pH 4.55 PO^- protonation, governed by $k_{off}^{D''}$, and subsequent D'' reprotonation, $k_{on}^{D''}$, are the only observable processes. Table VI collects the rate constants determined when PO^- protonation prevailed.

It is important to note that proton transfer to PO^- from any protonated dye could not be observed under any conditions in homogeneous solutions. Apparently, the close proximity of proton donors and acceptors on the positively charged micellar surface is an essential requirement for this process.

Conclusion

Data obtained in this work is consistent with the strong solubilization of the initially formed POH-CTAB complex by micelles. POH, however, remains in a relatively aqueous environment where its rotation is relatively free. Essentially a similar situation has been encountered in the interaction of rose bengal with aqueous micelles.[33] These data are, of course, consistent with current ideas about micellar structures which allow for extensive exposure of the hydrocarbon tails to water.[17]

The identical ground and excited state dissociation of POH in the absence and in the presence of micelles are the consequence of approximately equal retardation of both the protonation and deprotonation rates. These micellar retardation of proton-transfer rates are the consequence of altered microenvironments and electrostatic interactions. If dyes having appropriate pK_a values are solubilized in addition to POH on the micellar surface, the direction of the laser-initiated proton flow can be delicately tuned by altering the pH. Since each micelle contains less than one donor and acceptor, proton transfer must occur via solvent molecules.

Acknowledgment. Support of this work by NSF and ARO is gratefully acknowledged. We thank Mr. Wayne Reed for his continuous help in theoretical and practical matters. M. J. Politi thanks CNPq, Brazil, for a fellowship.

Registry No. POH, 27928-00-3; bromocresol green, 76-60-8; bromophenol red, 2800-80-8; bromothymol blue, 76-59-5; thymol blue, 76-61-9; pyranine, 6358-69-6.

(30) Sager, A.; Maryott, A. A.; Schooley, M. R. *J. Am. Chem. Soc.* **1948**, *70*, 732-736.
(31) "Lange's Handbook of Chemistry"; Dean, J. A., Ed.; McGraw-Hill: New York, 1979; pp 5-86.
(32) Mukerjee, P.; Banerjee, K. *J. Phys. Chem.* **1964**, *68*, 3567-3574.
(33) Reed, W.; Politi, M. J.; Fendler, J. H. *J. Am. Chem. Soc.* **1981**, *103*, 4591-4593.

Dissociation Dynamics of Energy-Selected Hexamethyldisilane Ions and the Heats of Formation of $(CH_3)_3Si^+$ and $(CH_3)_3Si$

Laszlo Szepes[†] and Tomas Baer*

Contribution from the Department of Chemistry, University of North Carolina, Chapel Hill, North Carolina 27514. *Received April 4, 1983*

Abstract: The photoelectron-photoion coincidence (PEPICO) technique has been used to investigate the unimolecular decomposition of the $(CH_3)_6Si_2^+$ molecular ion. The absolute rates of $C_3H_9Si^+$ and $C_5H_{15}Si_2^+$ ion formation were measured as a function of the internal energy by analyzing the ion time-of-flight distribution. The results are compared to the rates predicted by the statistical theory (RRKM/QET). The two dissociation channels are in competition with each other, and their observed onsets are subject to a considerable kinetic shift which is taken into account in evaluating the thermochemical dissociation limits. The rate data show that methyl loss is associated with a tighter transition state than the complex producing $C_3H_9Si^+$ ions. The $\Delta H_f°_{298}$ (in kJ/mol) for the following species were measured: Me_3Si (-49); Me_4Si (-226.2); Me_3Si^+ (629.7); $Me_2Si_2^+$ (423). A Si-Si bond energy of 265 kJ/mol is derived from the heat-of-formation data.

The trimethylsilyl ion is particularly important in the mass spectrometry of methylsilanes, polymethylsilanes, and siloxanes as well as silylated compounds.[1] This ion has been investigated by several authors, and its thermochemistry has been the subject

[†] Department for General and Inorganic Chemistry, Eötvös Loránd University, Budapest, Hungary.

(1) Litzow, M. R.; Spalding, T. R. In "Mass Spectroscopy of Inorganic and Organometallic Compounds"; Elsevier, Amsterdam, 1973; Chapter 7.

0002-7863/84/1506-0273$01.50/0